PROCEEDINGS, 45th Workshop on Geothermal Reservoir Engineering
Stanford University, Stanford, California, February 10-12, 2020
SGP-TR-216

Possibility of high Vp/Vs zone in the geothermal field suggested by the P-to-S conversion

Junzo Kasahara[1,2], Yoko Hasada[1,3] and Haruyasu Kuzume[1]

[1]ENAA Toranomon Marine Building 10th, 3-18-19 Toranomon, Minato-ku, Tokyo 105-0001

[2] Shizuoka Univ., Center for Integrated Research and Education of Natural Hazard, 836 Ohya, Shizuoka, Japan

[3] Daiwa Exploration and Consulting Co. Ltd., 5-10-4 Toyo, Koto, Tokyo, Japan

Kasahara.junzo@shizuoka.ac.jp

Keywords: P-to-S conversion, high *Vp/Vs* ratio, Poisson's ratio, geothermal reservoir, water saturation, temperature effects, supercritical water

ABSTRACT

To develop effective tools to describe the characteristics of geothermal fields, we conducted a seismic observation using fiber-optic distributed acoustic sensors (DASs) and ground surface seismometers in November 2018. We performed the seismic study at the Medipolis geothermal field in the southern part of Kyushu, Japan. We deployed a fiber-optic cable for the DASs at a depth of 977 m in the IK-4 well and installed 20 sets of 3C ground surface geophones that exhibit unusual waveform characteristics. Although the amplitudes of the first arriving P-waves in some earthquakes on UD geophones are small, the EW and NS geophones exhibit weak P first arrivals and successive intense phase with a delay of 0.8 s. When we assume the *Vp/Vs* = 3 zone at a depth of 4 km with a thickness of 500 m, the models can explain the observed characteristics. We concluded that this phase is the P-to-S converted phase. We also examined the detectivity of any high *Vp/Vs* reservoir using the full-waveform inversion (FWI) method. FWI suggests that we can retrieve the location and shape of zones with high *Vp/Vs*. The 2019 seismic study in the same geothermal field yielded a reflection corresponding to a depth of approximately 3.6 km, suggesting a high *Vp/Vs* zone. *Vp/Vs* = 3 cannot be explained by temperature effects, but it can be explained by high water saturation. *Vp/Vs* = 3 corresponds to the Poisson's ratio of 0.467. Considering that the Poisson's ratio of water is 0.5, the high *Vp/Vs* zone could be at the supercritical state of water.

1. INTRODUCTION

To develop a smart technology to characterize super-critical reservoir(s), we proposed a hybrid method to use ultra-stable seismic sources, distributed acoustic sensors (DASs), ground surface geophones, and the full-waveform inversion (FWI) method (Kasahara *et al*., 2019a). To evaluate the effectiveness of this approach in an operating geothermal field, we conducted a seismic study at the Medipolis geothermal field in southern Kyushu, Japan.

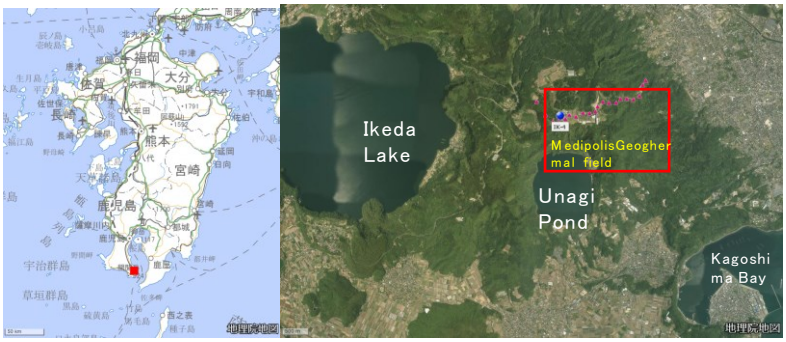

Figure 1: (Left) Kyushu island and the Medipolis geothermal field (red square). (Right) Medipolis geothermal field at the upper right. The IK-4 well is indicated by a blue dot and the ground surface geophones are indicated by red triangles. The ground surface geophone spacing is 100 m. The maps are from GSJ.

Medipolis is located in the Ibusuki geothermal area, Japan (Fig. 1). There are three geothermal wells in the field. The geothermal characteristics, such as temperature, lithology and chemistry of the wells, were studied by NEDO (2008–2010). The IK-1 well is commercially used to generate 1.4 Mw of electric power using the binary system. The IK-3 is a reduction well. We used the IK-4 well for this study. The depths of the three wells are approximately 1,500 m. The temperature of the wells around a depth of 900 m was approximately 250 °C, and steam was observed at a depth of approximately 1,300 m. The temperature model by NEDO (2008–2010) proposed the presence of a hot reservoir around the NE direction of IK-1 and IK-4 wells; however, it has not been confirmed by real drillings.

To determine the precise *Vp* and *Vs* structures and hot water distribution in this field, we conducted a seismic observation using fiber-optic DASs and ground surface geophones in November 2018 (Kasahara *et al*., 2019b)

2. FIELD STUDY AND OBSERVED RESULTS

We installed a fiber-optic cable for the measurements using DASs and distributed temperature sensors (DTSs) at a depth of 977 m and 20 sets of 3C geophones along the 2 km-long EW line (Fig. 1). We measured the temperature and seismic signals using the same fiber-optic cable for DASs and DTSs. The temperature of IK-4 was measured to be 264 °C by the DTSs at 914 m. The interval of ground surface geophones was approximately 100 m. We observed seven natural earthquakes via DASs and ground surface geophones for four and a half days (Table 1 and Fig. 2). The largest observed earthquake was M = 5.2, which occurred west of Tanegashima with a focal depth of 123 km ("A" in Fig. 2). Fig. 3 shows the records of the DASs and ground surface geophones for the M = 5.2 earthquake (EQ5 in Table 1).

Table 1: List of earthquakes observed by DASs for four and a half days.

	Origin time	Latitude	Longitude	Depth(km)	Magnitude	Area
EQ1	2018/11/20/03:16 28.7	31° 23.6'N	130° 37.1'E	10	1.4	C
EQ2	2018/11/20/19:34 52.2	29° 21.5'N	129° 48.4'E	65	4	D
EQ3	2018/11/20/22:02 42.3	31° 24.2'N	130° 34.3'E	14	0.9	C
EQ4	2018/11/20/23:09 01.5	31° 30.0'N	130° 42.4'E	119	2.3	E
EQ5	2018/11/21/04:09 49.9	30° 24.0'N	130° 9.0'E	123	5.2	A
EQ6	2018/11/21/04:59 29.1	30° 26.9'N	130° 9.1'E	123	3.1	B
EQ7	2018/11/21/17:49 18.0	31° 19.3'N	131° 42.7'E	22	2.7	F

On observing the seismic records of 3C ground surface geophones, we identified large amplitude arrivals observed approximately 0.8 s after the P first arrivals on the NS and EW components, even though the UD component exhibited only weak P first arrivals, as evident in Fig. 3. DAS records did not show similar phases and S arrivals because the incident angles of the observed earthquakes, listed in Table 1, were near vertical, and the DASs detected vibrations along the fiber elongation. Another similar phase as Fig. 3 is shown in Fig. 4 for EQ2.

Figure 2: Earthquakes observed by DASs for four and a half days (stars). Blue circles denote the location of DASs at the Medipolis field.

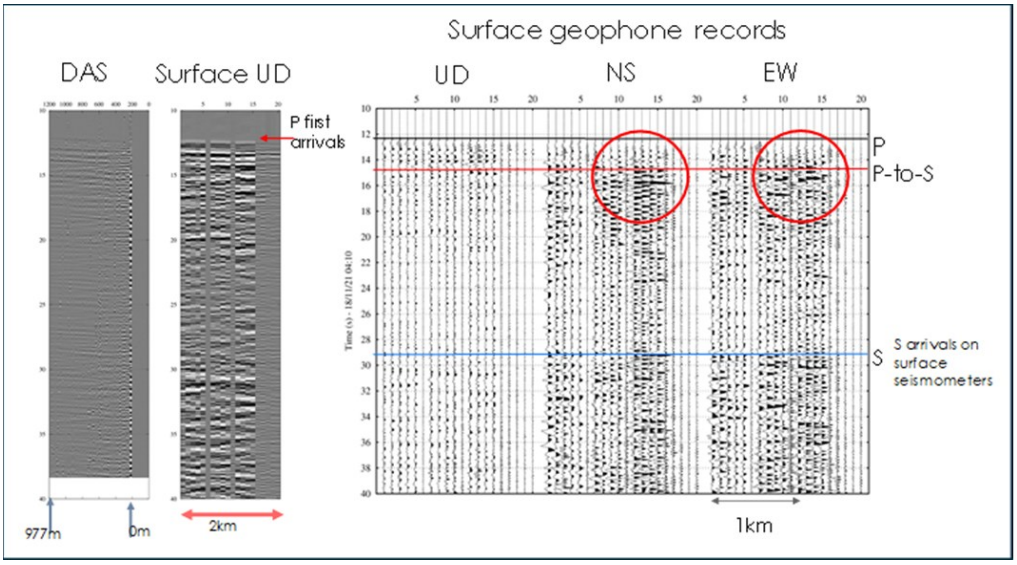

Figure 3: Possible P-to-S conversion arrivals seen in EQ5 observed by the ground surface geophones. (Far left) DASs records. The vertical axis denotes the arrival time in seconds and the horizontal axis denotes the distance. (Middle) UD component of ground surface geophones. (Far right) Ground surface geophone records of UD, NS, and EW components. Each ground surface seismic station is located at 100 m spacings. Large amplitude arrivals are recognized in the NS and EW components approximately 0.8 s after the first P arrivals observed in the UD component records.

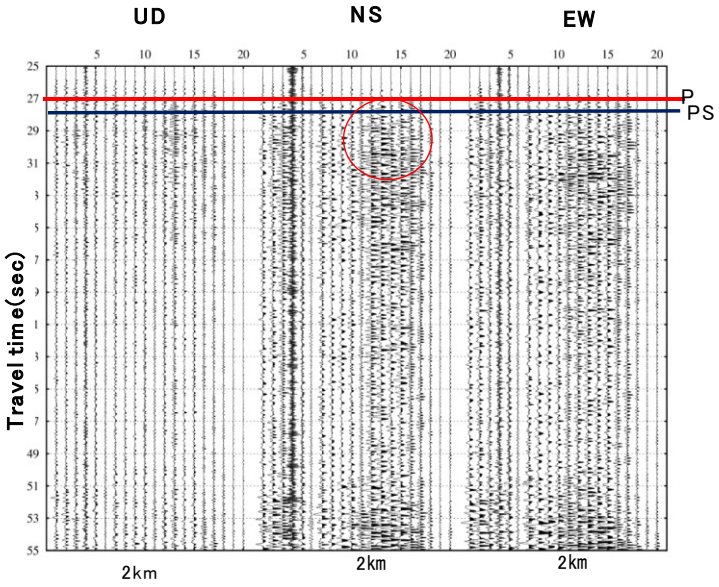

Figure 4: P-to-S conversion for the earthquake, i.e., EQ2 (M=4.0) ("D" in Fig. 2). The time delay in P-to-S converted phase from P first arrival is approximately 0.8 s. The vertical axis denotes the travel time.

3. FORWARD MODELING TO EVALUATE P-TO-S CONVERSION

Such characteristics, as shown in Figs. 3 and 4, were frequently observed in the marine seismic study; they are the P-to-S converted phases at the soft marine-sediment (Kasahara *et al*., 1982). When P waves penetrate from a hard rock base into soft marine sediments, the P-to-S conversion occurs. The P-to-S converted phase is delayed by ~2 s and large amplitudes form thick marine sediments. In the ocean floor, the value of *Vp* of the hard rock base is approximately 3.5–6 km/s, and the *Vp* and *Vs* of the marine sediments are ~2 km/s and 100–300 m/s, respectively. In the Medipolis geothermal field, the *Vp* is approximately 3–4 km/s between a depth of 200 and 1000 m (Kasahara *et al.* 2019b) and *Vp/Vs* is considered to be 1.75 for most of the surrounding layer.

We examined the cause of the estimated P-to-S conversion at the Medipolis geothermal field. The delay time from the P first arrival to the P-to-S converted phase is estimated to be ~0.8 s. We assumed a *Vp/Vs* = 3 zone at a depth of 4 km with a thickness of 500 m (Fig. 5) and calculated the theoretical waveforms generated by deep seismic sources corresponding to the plane wave incident at a depth of 5 km. The seismic velocity profile estimated by the DAS observations was used in the calculation (Kasahara *et al*., 2019b).

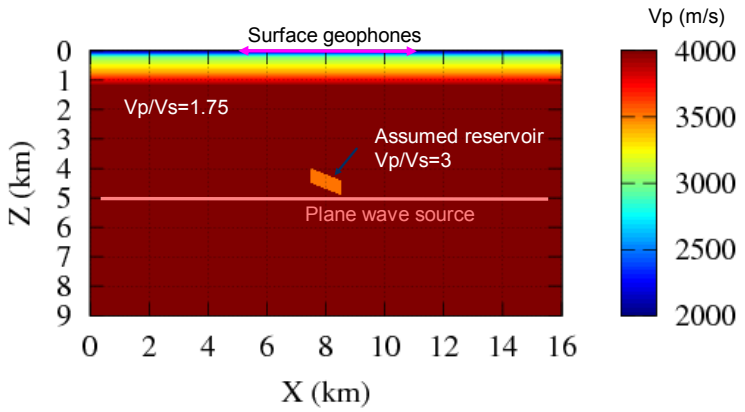

Figure 5: Model to examine the P-to-S conversion. *Vp/Vs* in the reservoir is assumed to be 3. The plane wave source at 5 km depth. The dip of the reservoir is 20°.

The calculated waveform for the model (Fig. 5) is shown in Fig. 6. The P-to-S converted phase is evident on the horizontal component of the 4 km-deep reservoir. The vertical component shows intense P first arrivals and weak scattered P.

To examine the amplitude of the P-to-S conversion, we extracted the waveforms at 8.8 km (shown in Fig. 7). The weak P first arrival and successive intense P-to-S conversion arrival were observed on the horizonal component. In contrast, the vertical component shows only P arrival. The calculated waveforms can explain the observed characteristics, such as weak P first arrivals and intense P-to-S converted phases on the horizontal components, when the incident seismic wave is slightly oblique to the high *Vp/Vs* zone. We also estimated waveforms in the well and ground surface.

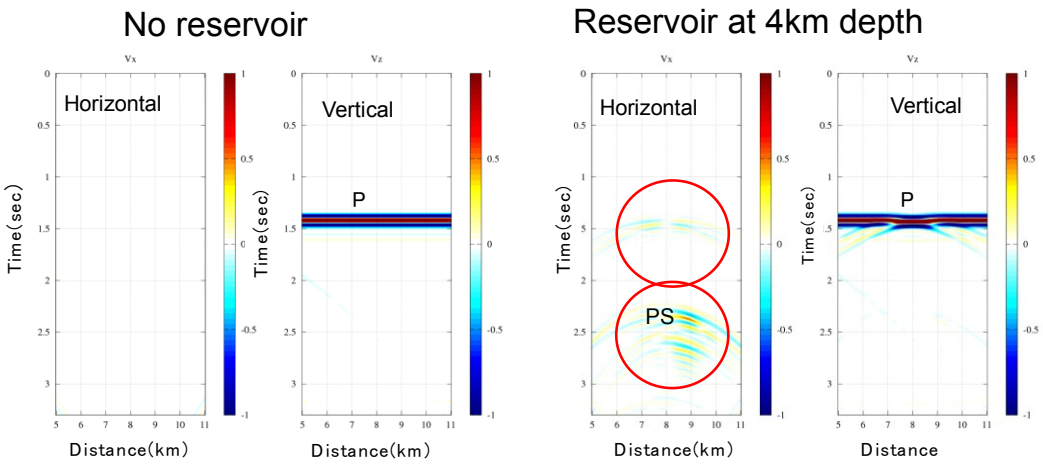

Figure 6: Calculated waveforms of ground surface geophones using the model shown in Fig. 3. Incident wave is assumed as plane wave at a depth of 5 km. Horizontal axis: distance (km) and vertical axis: travel time (sec). (Left two) no reservoir case. (Right two) presence of a 4 km-deep reservoir (Fig. 5).

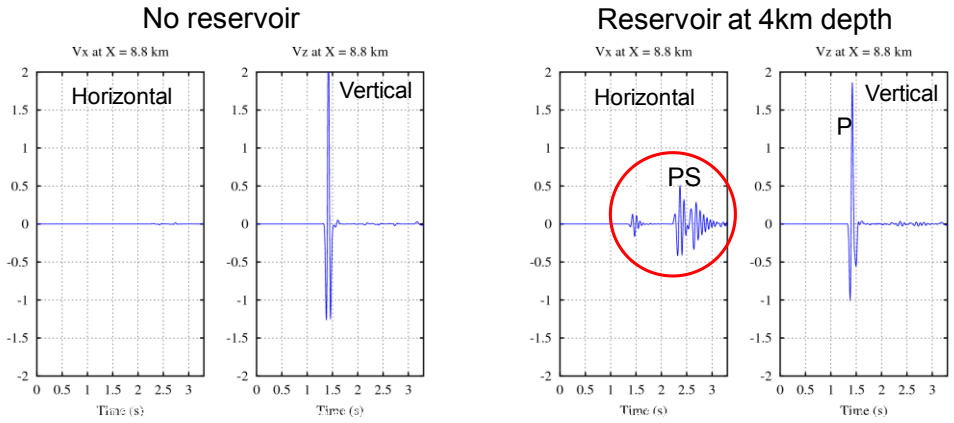

Figure 7: Waveforms at 8.8 km from the left edge of the model shown in Fig. 5. It is noted that the P-to-S conversion arrival is observed on the horizontal component, but only intense P first arrival is seen on the vertical component for the 4 km-deep reservoir model.

3. FWI examination

To examine the possibility of the presence of the reservoir causing P-to-S conversion, we used the FWI approach. Several papers have examined the FWI methods for seismic reflection seismology (*e.g.*, Tarantola, 1984, 1986; Virieux and Operto, 2009; Tromp *et al*., 2005; Alkalifah, 2016; Schuster, 2017). We used the "adjoint methods" proposed by Tromp *et al.* (2005) (Kasahara *et al.*, 2019a).

The model for the FWI calculation is shown in Fig. 8. The model is a more realistic case reflecting the geographical conditions of Medipolis. We used a vertical single force applied at 6 km from the left side. The DASs in the well and ground surface geophone array are assumed to be installed at the Medipolis geothermal field. However, we considered the horizontal components using the DASs because a helical fiber will be introduced in the near future.

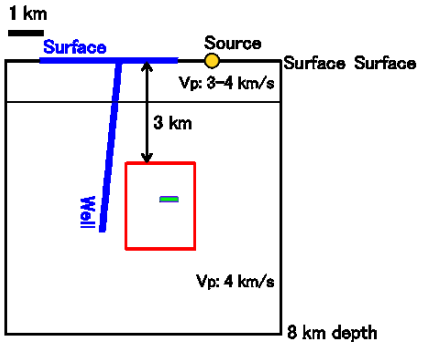

Figure 8: FWI model to evaluate the field study on whether a 4 km-deep reservoir can be detected by a P-to-S conversion. (Green rectangle) A 500 m-long and 100 m-thick rectangular reservoir is located at a depth of 4 km. No density change is assumed. (Yellow circle) A vertical single force is applied at 6 km from the left edge of the model. *Vp/Vs* = 3 in the assumed reservoir. The red rectangle shows the area used by the FWI calculation.

The model for the FWI calculation is shown in Fig. 8. The model is a more realistic case reflecting the geographical conditions of Medipolis. We used a vertical single force applied at 6 km from the left side. The DASs in the well and ground surface geophone array are assumed to be installed at the Medipolis geothermal field. However, we considered the horizontal components using the DASs because a helical fiber will be introduced in the near future.

The synthetic residual waveforms created by the assumed reservoir at a depth of 4 km is illustrated in Fig. 9. In the FWI simulation, we used synthetic residual waveforms before the presence of the 4 km-deep reservoir, as shown in Fig. 10 because we assumed time lapse. The PP and PS reflections can be observed at a depth greater than 3 km by the DASs in the well. PP, PS, and SS reflections appeared by the ground surface geophone at approximately 3–5 km.

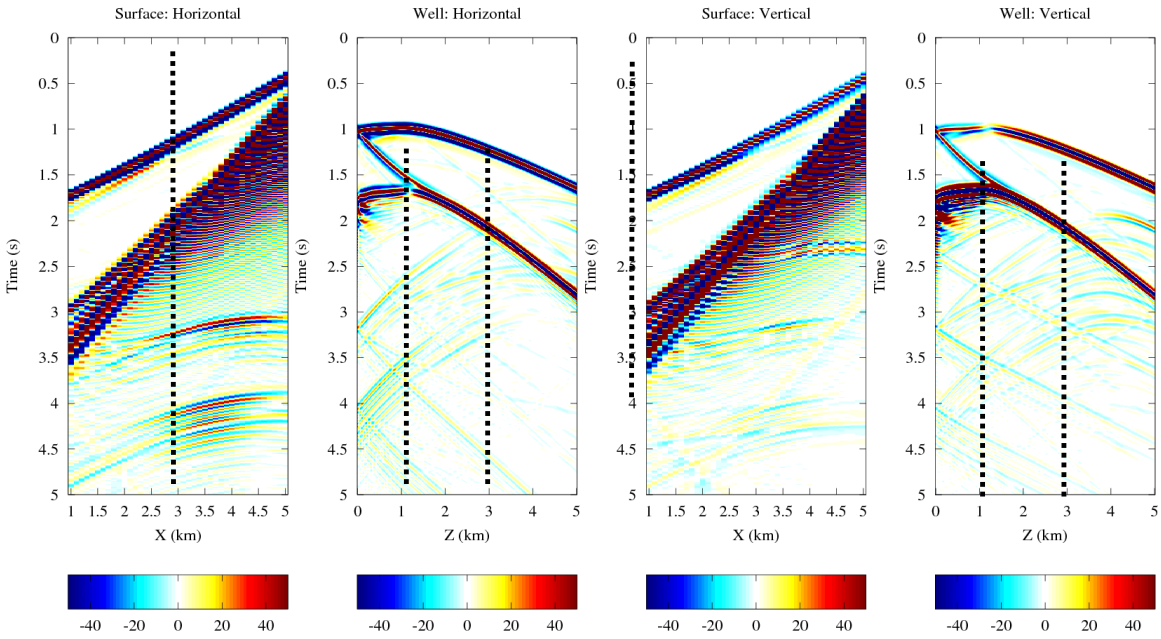

Figure 9: Synthetic waveforms for the model shown in Fig. 8. A vertical single-force is applied. From left to right: Horizonal component at surface, horizontal component in the well, vertical component at surface, and vertical component in the well.

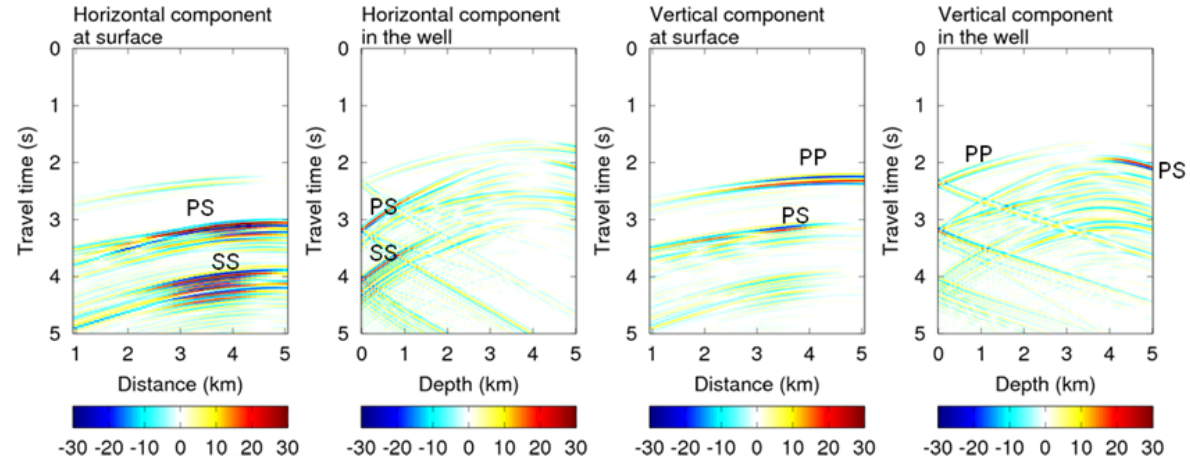

he

Figure 10: Residual waveforms in the wells and ground surface geophones between the uniform initial model and true model of FWI. Relatively small P and large PS phases are observed in the horizontal components. *Vp/Vs* = 3 in the reservoir, which is obtained by forward modeling to generate the P-to-S conversion. PP, PS, and SS reflected phases are observed in the reservoir. PP, PS, SS are reflected phases at the reservoir.

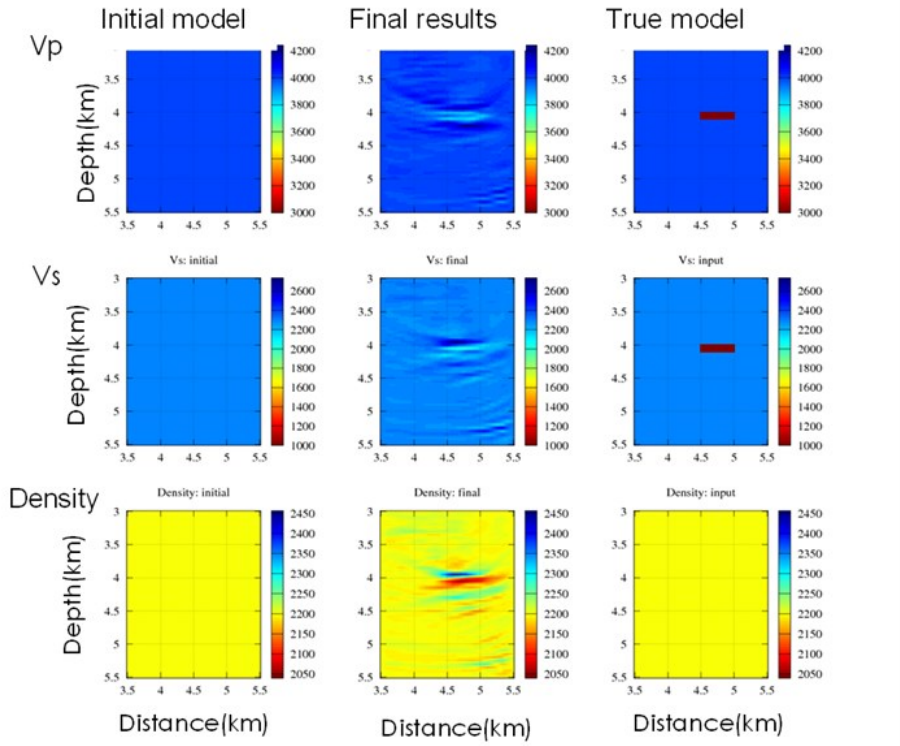

Figure 11: Result of the first stage is shown in the central column. The true model is shown in the right column. The initial model is shown in the left. No density change is assumed.

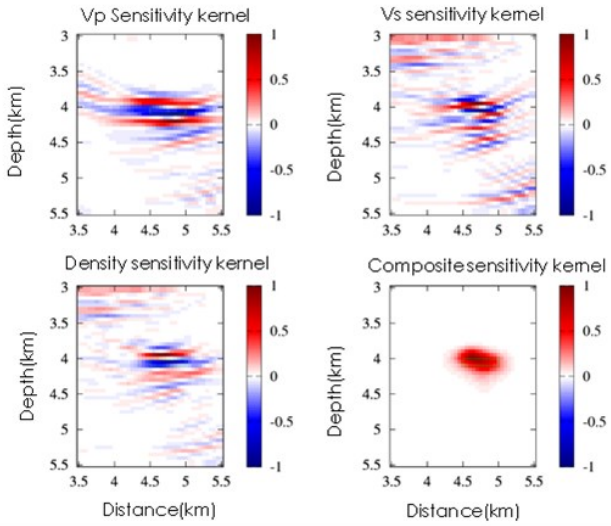

Figure 12: Sensitivity kernels at the first stage of the FWI model. By combining the three sensitivity kernels, we develop the location and shape of the second stage, as shown at the bottom right.

We applied two stages for the inversion. The first stage mainly focused on the location and shape. Fig. 11 shows the result of the first stage. The location of the assumed reservoir appears to be well retrieved. Using the results of the sensitivity kernels in the first stage shown in Fig. 12, we created the second stage model. The result is shown in Fig. 13. The results demonstrated reasonable location and shape of the assumed reservoir, but the assumed physical properties were not well-retrieved.

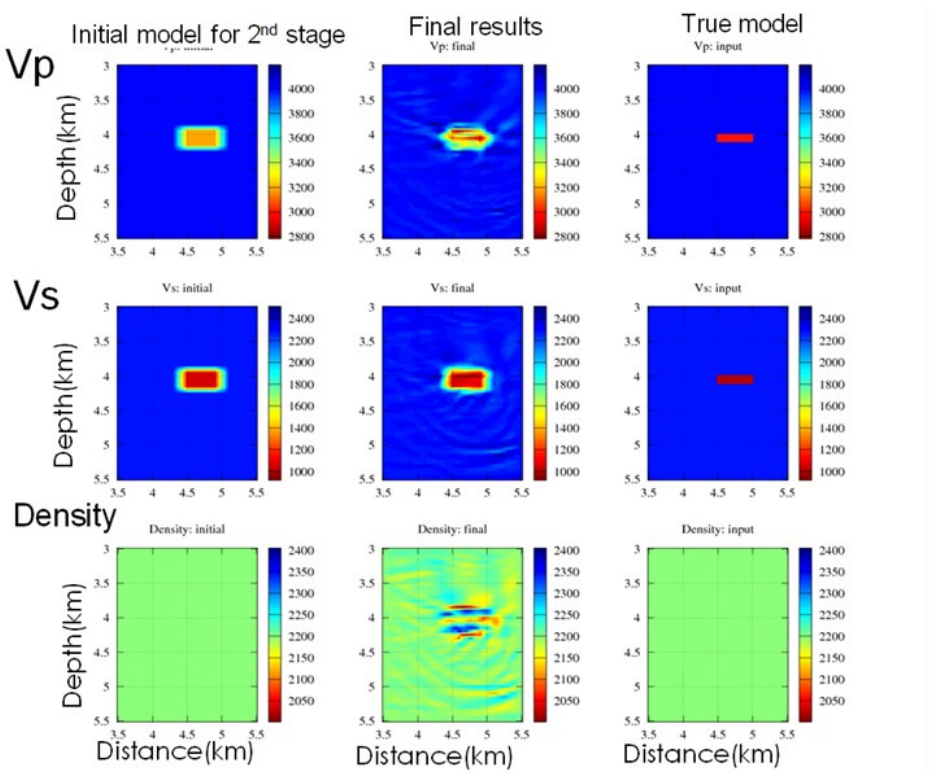

Figure 13: Result of FWI calculation is shown in the central column. The true model is shown in the right column. The initial model of the second stage is shown in the left column.

4. DISCUSION AND CONCLUTION

During the seismic study at the Medipolis geothermal field, a distinct phase was observed by the horizonal component of the ground surface geophones. We considered this phase to be the P-to-S converted phase and examined this possibility. By calculating the theoretical seismograms assuming the *Vp/Vs* = 3 zone at a depth of 4 km with 20° dip angle, we obtained similar waveforms as those observed by ground surface geophones.

We also evaluated the possibility to detect any P-to-S converted origin using the FWI method. We assumed a high *Vp/Vs* zone at a depth of 4 km with thickness of 500 m. The FWI suggests that we can retrieve the location and shape of high *Vp/Vs* zones if we use the combination of active seismic source(s), the DASs in the well, and the ground surface geophones. However, the physical properties of the assumed reservoir were not fully retrieved. Because the current FWI model reflects more realistic field conditions like those in Medipolis, the limited aperture of the observed system might cause poor retrieval of the physical properties. The previous FWI modeling assuming a more idealistic DAS system yielded good physical properties (Kasahara *et al*., 2019a). The seismic study at the same geothermal field in 2019 suggested the presence of high *Vp/Vs* zones at a depth of approximately 4 km (Kasahara *et al*., 2020). The DAS-VSP works in the same Medipolis geothermal field in 2019 exhibited several distinct upgoing phases. By forward modeling and migration of upward phases, we determined that the *Vp/Vs* = 3 zone is required at a depth of 3.6 km (Kasahara *et al*., 2020). Although the depth of high *Vp/Vs* zones obtained by the present P-to-S conversion analysis is slightly greater than 3.6 km, the discrepancy between the two analyses can be explained by the uncertainty near surface *Vs* distribution.

We considered the meaning of *Vp/Vs* = 3. Using the numerous *Vp* and *Vs* measurements under high pressure and temperature by Kern (1978), Kern and Richter (1981), and Kern *et al.* (1997), most quartz free rocks showed very small temperature dependence of *Vp* and *Vs*. Rocks including quartz minerals demonstrated large temperature dependence on *Vp* due to that phase change from α to β quartz (Kern and Richter, 1981). For quartz free rocks, *Vp/Vs* remained constant to be approximately 1.75 and *Vp/Vs* = 3 was not explained. The serpentine rock exhibited large decreases in *Vs* and *Vp* at temperatures higher than 500 °C (Kern and Richter, 1981). The amount of velocity decrease at high temperature was explained by the dehydration of antigorite, which is a high temperature-type serpentine mineral. The velocity decrease in *Vs* was larger than that in *Vp*. Water saturation in rocks might be a cause of high *Vp/Vs*.

In addition, the *Vp/Vs* is related to the Poisson's ratio "ν" by the following equation.

$$\nu = \frac{1}{2}\frac{(V_P/V_S)^2 - 2}{(V_P/V_S)^2 - 1}$$

Using the above equation, *Vp/Vs* = 3 corresponds to 0.467 for the Poisson's ratio. Because the Poisson's ratio of water is 0.5, the suggested zone at a depth of approximately 3.6–4 km could be filled by water. Winlker and Nur (1985) obtained *Vp/Vs* > 2 for the Massillon sandstone if the sandstone was 100% saturated by water.

Considering the above discussion, high *Vp/Vs* suggests the presence of high-water saturation zones at a depth of approximately 4 km. Because the temperature at the depth of 914 m is 264 °C in the IK-4 well, the zone around 4 km depth might be close to the supercritical state if the zone is filled by water.

ACKNOWLEDGHMENTS

This article is based on the results obtained from a project commissioned by the New Energy and Industrial Technology Development Organization (NEDO).

REFERENCES

NEDO: Report of Geothermal Development Promotion, East of Ikeda Lake No. C-2-10, First, Second and Third phases, (2008, 2009, 2010).

Kasahara, J., Nagumo, S., Koresawa, S., Nishi, Y., and Sugimoto, H.: A linear trend of hypocenter distribution in the outer slope region of the Japan Trench revealed by the OBS array-Preliminary report- Bull. Earthq. Res. Inst., Univ. Tokyo, **57,** (1982), 83-104.

Kasahara, J., Hasada, Y., and Yamaguchi, T.: Seismic imaging of supercritical geothermal reservoir using full-waveform inversion method, *Proceedings*, 44th Workshop on Geothermal Reservoir Engineering, Stanford University, Stanford, CA (2019a).

Kasahara, J., Hasada, Y, Kuzume, H., Fujise, Y. and Yamaguchi, T. Seismic feasibility study to identify supercritical geothermal reservoirs in a geothermal well using DTS and DAS, EAGE extended abstract, EAGE 2019 Annual meeting, London (2019b).

Kasahara, J., Hasada, Y., Kuzume, H., Mikada, H., and Fujise, Y.: The second seismic study at the geothermal field in southern Kyushu, Japan using an optical fiber system and surface geophones, *Proceedings*, 45th Workshop on Geothermal Reservoir Engineering, Stanford University, Stanford, CA (2020).

Kern, H.: The effect of high temperature and high confining pressure on compressional wave velocities I quartz-bearing and quartz-free igneous and metamorphic rocks, Tectonophysics, **44**, (1978), 185-203.

Kern, H., and Richter, A.: Temperature derivatives of compressional and shear wave velocities in crust and mantle rocks a 6 kbar confining pressure, Jour. Geophys., **49,** (1981), 47-56.

Kern, H., Liu, B., and Popp, T.: Relationship between anisotropy of P and S wave velocities and anisotropy of attenuation in serpentine an amphibolite, Jour. Geophys. Res. **102**(B2), (1997), 3051-3065.

Schuster, G. T.: Seismic inversion, Investigations in geophysics. No. 20, SEG (2017)

Tarantola, A.: Inversion of seismic reflection data in the acoustic approximation, Geophysics, **49**, (1984), 1259-1266.

Tarantola, A.: A strategy for nonlinear inversion of seismic reflection data, Geophysics, **51**(10), (1986), 893-1903.

Tromp, J, Tape, C., and Liu, Q.: Seismic Tomography, Adjoint Methods, Time Reversal and Banana-Doughnut Kernels, Geophysical Journal International 160.1 (2005), 195-216.

Virieus, J. and Opeto, S.: An overview of full-waveform inversion in exploration geophysics, Geophysics, **74**, (2009), WCC1-WCC26.

Winkler, K. W., and Nur, A.: Seismic attenuation: effects of pore fluids and frictional sliding, Geophysics, **4,** (1982), 1-15.